Isothermal crystallization of poly(ethylene-terephthalate) of low molecular weight by differential scanning calorimetry:

1. Crystallization kinetics

P. Colomer Vilanova and S. Montserrat Ribas
Departmento de Termodinámica y Fisicoquímica, E. T. S. Ingenieros Industriales de Terrassa (U. P. B.) Colón, 11 Terassa. (Barcelona), Spain

and G. Martin Guzman
Departmento de Química Física, Facultad de Ciencias Químicas de San Sebastián, Universidad del País Vasco. Alza, San Sebastián, Spain

(Received 2 April 1984; revised 10 September 1984)

The isothermal crystallization of poly(ethylene-terephthalate) (PETP) fractions, from the melt, was investigated using differential scanning calorimetry (d.s.c.). The molecular weight range of the fractions was from 5300–11750. Crystallization temperatures were from 498–513 K. The dependence of molecular weight and undercooling on several crystallization parameters has been observed. Either maxima or minima appear at a molecular weight of about 9000, depending on the crystallization temperature. The activation energy values point to the possibility of different mechanisms of crystallization according to the chain length. A folded chain process for the higher $\bar{M}_n$ chains and an extended chain mechanism for the lower $\bar{M}_n$ chains. The values of the Avrami equation exponent n vary from 2–4 depending on the crystallization temperature; non-integer values are indicative of heterogeneous nucleation. The rate constant K depends on T_c and $\bar{M}_n$, showing maxima related to the T_c used. The plot of log K either vs. $(\Delta T)^{-1}$ and $(\Delta T)^{-2}$ or $T_m/T(\Delta T)$ and $T_m^2/T(\Delta T)^2$ is linear in every case.

(Keywords: poly(ethylene-terephthalate); crystallization; d.s.c.; kinetics; undercooling)

INTRODUCTION

The kinetics and thermodynamics of polymer crystallization is nowadays a subject of considerable importance[1-2]. Several techniques are widely employed, such as dilatometry[3-10], calorimetry[11-17], microscopy[18-20], light depolarization and scattering[21], density[22], etc., according to the parameters implied in the processes studied. In particular, differential scanning calorimetry has proved to be a convenient technique because of the small size of sample required, speed of operation and possibility of quickly reaching thermal equilibrium. It has been shown that the results obtained by d.s.c. are comparable to those from dilatometry[23,24], with larger undercoolings and, therefore, higher crystallization rates.

On the other hand, it is well known that most of the parameters involved in crystallization phenomena depend on the temperature of crystallization, T_c, and the molecular weight[25-31]. For this reason the use of well fractionated samples is a necessary condition. For a given undercooling, the crystallization rate is closely associated to two energy quantities; that is, nucleation free energy and the one belonging to the transport at the interface liquid-crystal. The free energy of nucleation is independent of molecular weight beyond a certain value and the crystallization rate will depend only on the transport term and therefore of the molecular weight which determines the environmental viscosity. As the crystallization temperature decreases followed by smaller nuclei and concentration of chain units required for nucleation, the influence of molecular weight becomes less important[14,25,32,33]. It is necessary for this reason that the polymer fractions employed cover a wide range of molecular weights; to find out in each system what the influence is that the molecular weight has on each of the energy terms.

During the last years a number of papers have been published with reference to the effect of molecular weight on the various kinetics variables, and a few of them make reference to low molecular weight values[27,34,35]. With regard to poly(ethylene-terephthalate) this is not the case, however, and currently attention has been paid mainly to the higher molecular weight range[36-45].

The purpose of this investigation has been to study the effect of the molecular weight as well as of the undercooling on the kinetic parameters associated with the poly(ethylene-terephthalate) crystallization from melt, paying particular attention to the low molecular weights. D.s.c. was used, and the molecular weights of the fractions used, varied from 5300–11 750. In a paper to follow, the temperature coefficient and associated parameters of this crystallization will be reported.

0032-3861/85/030423-06$03.00

EXPERIMENTAL

Samples

In this work we used several low molecular weight fractions of PETP, with $\bar{M}_n$ in the range 5300–11 750. Fractionation was carried out by the temperature lowering technique from solutions in *N*-*N*-dimethylformamide (DMF). The original PETP sample unfractionated has been prepared by polycondensation of ethylene glycol and dimethyl-terephthalate in the presence of antimonium trioxide and calcium acetate. Molecular weight determinations have been carried out by intrinsic viscosity measurements in *o*-chlorophenol at 25°C. Details regarding the synthesis, fractionation and characterization of samples have been reported in a previous paper[46].

ISOTHERMAL CRYSTALLIZATION

The kinetics of isothermal crystallization were determined using a Perkin-Elmer DSC-1B instrument operating in nitrogen atmosphere. Temperature calibration was carried out using pure samples of In, Sn and Pb. The apparent enthalpies were determined using the conventional method, comparing the areas under the d.s.c. curve with the corresponding areas of a standard sample of Indium, taking $\Delta H_f = 28.45\ \mathrm{J g^{-1}}$.

The crystalline content was determined by comparison of the apparent enthalpies with those of a 100% crystalline sample which is 120 $\mathrm{J g^{-1}}$ according to Roberts[47].

Kinetic experiments have been performed following the usual method[14]. The samples were heated to a temperature T_f, about 20°C above the corresponding melting temperature, standing at that temperature for a time t_f until the complete disappearance of any residual crystallinity in the melt. Previous trials carried out with the different fractions allowed us to determine fusion conditions at 548 K and 5 min, respectively. These conditions were used in all the experiments. Subsequently, the samples were cooled at a rate of 64°C $\mathrm{min^{-1}}$ until the desired crystallization temperature was reached and the corresponding crystallization exotherms scanned as a function of time, until no change was observed.

Once crystallization had been completed, to obtain the melting temperature as well as the corresponding enthalpy the samples were heated at 8°C $\mathrm{min^{-1}}$ until total fusion took place. The crystallization temperatures used to evaluate kinetic data are in the range 498–513 K for the fractions.

RESULTS

The induction time τ_i has been found from the d.s.c. curves, taking τ_i as the distance from the point of thermal equilibrium to the starting point of the isotherm (*Figure 1*). It must be taken into account that τ_i is not a proper induction time as the initiation of the exotherm does not guarantee that the crystalline content is zero in that moment. In addition, as the crystallization temperature is lowered the rate of crystallization increases and the true initial point of the exotherm may be not detectable as a result of the incomplete thermal equilibrium attained.

Apparent induction times, for each fraction and crystallization temperature, are listed in *Table 1*. *Figure 2* shows

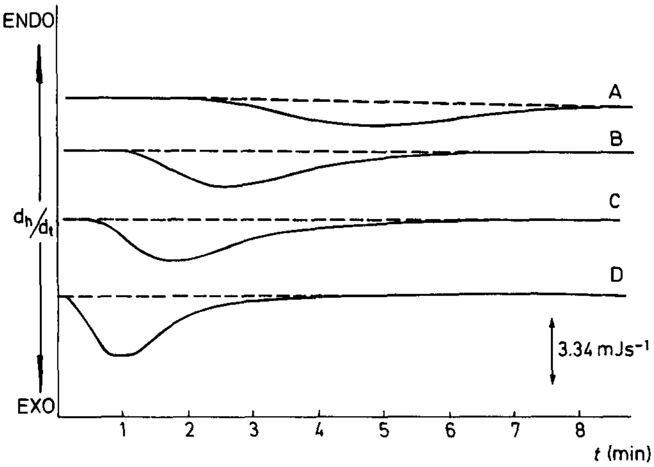

Figure 1 D.s.c. curves for fraction *A*-1 (M_n=11750). Melting conditions: 548 K and 5 min. Curve A: τ_i=2.1 min, T_c=508 K; curve B: τ_i=0.9 min, T_c=505 K; curve C: τ_i=0.5 min, T_c503 K; curve D: τ_i=0.1 min, T_c=500 K

Table 1 Crystallization parameters for each fraction. Melting conditions: 548 K and 5 min

Fraction	T_c(K)	τ_1(min)	v_c(min^{-1})	$t_{0.5}$(min)	$t_{0.1}$(min)	K(min^{-n})	n	K equation (6)	X%
A–0	508	2.60	0.194	5.82	3.80	1.46×10^{-3}	3.4	1.73×10^{-3}	46.1
Unfractionated	503	0.40	0.430	1.86	1.15	1.05×10^{-1}	3.1	1.01×10^{-1}	65.1
(M_n = 6650)	500	0.05	0.613	1.20	0.48	4.95×10^{-1}	2.6	4.31×10^{-1}	64.6
A–1	508	2.10	0.280	4.95	3.42	2.32×10^{-3}	3.9	1.35×10^{-3}	57.6
(M_n = 11750	505	0.90	0.356	2.95	1.76	1.64×10^{-2}	3.4	1.75×10^{-2}	66.4
	503	0.50	0.418	2.22	1.24	4.88×10^{-2}	3.4	4.60×10^{-2}	71.2
	500	0.10	0.558	1.22	0.50	4.23×10^{-1}	2.6	4.13×10^{-1}	69.4
A–2	513	6.80	–	13.80	–	–	–	–	–
($\bar{M}_n$ = 8100)	508	1.45	0.342	4.08	2.82	2.5×10^{-3}	4.0	2.50×10^{-3}	54.5
	505	0.60	0.520	2.10	1.32	9.76×10^{-2}	3.9	3.83×10^{-2}	52.6
	503	0.40	0.668	1.47	0.86	1.85×10^{-1}	3.4	1.87×10^{-1}	58.5
	500	0.20	0.955	0.77	0.35	1.420	2.4	1.297	61.6
A–3	508	2.15	0.258	5.47	3.75	7.74×10^{-4}	4.0	7.74×10^{-4}	58.4
(M_n = 7100)	505	0.85	0.432	2.73	1.73	1.35×10^{-2}	3.8	1.52×10^{-2}	64.2
	503	0.45	0.495	1.87	1.08	9.73×10^{-2}	3.1	9.95×10^{-2}	71.4
	500	–	0.716	0.97	0.45	8.02×10^{-1}	2.6	7.50×10^{-1}	72.0
A–4	508	4.90	–	–	–	–	–	–	–
($\bar{M}_n$ = 5350)	505	1.90	0.124	7.35	4.05	7.32×10^{-4}	3.5	6.43×10^{-4}	57.2
	500	0.30	0.344	2.31	1.15	4.37×10^{-2}	3.3	4.37×10^{-2}	58.7
	498	–	0.481	1.35	0.55	3.63×10^{-1}	2.0	3.80×10^{-1}	68.8

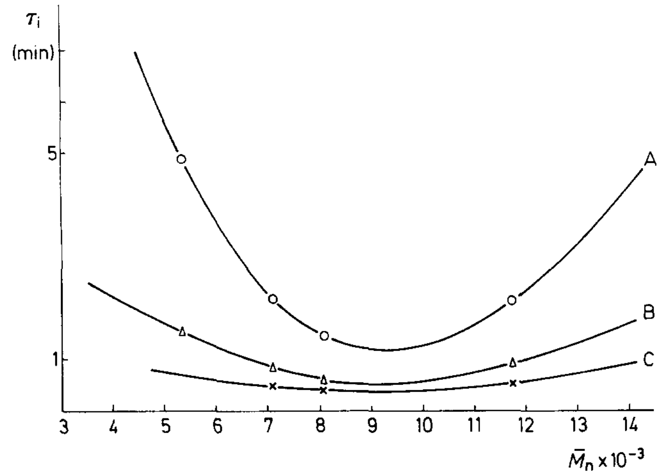

Figure 2 The induction time τ_i dependence on the molecular weight for various crystallization temperatures T_c. Curve A: T_c=508 K; curve B: T_c=505 K; curve C: T_c=503 K

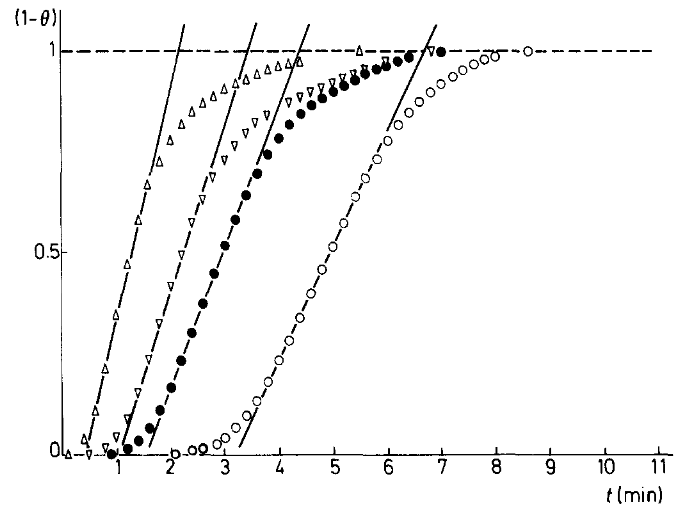

Figure 3 Reduced crystallinity as a function of time plot for fraction *A*-1. Crystallization temperatures: (△) 500 K, (▽) 503 K, (●) 505 K, (○) 508 K

the dependence of τ_i with M_n for various crystallization temperatures. A minimum, corresponding to a molecular weight of about 9000, can be seen.

The weight fraction of crystalline material $x(t)$ at time t has been calculated according to the equation:

$$x(t) = \int_0^t (\mathrm{d}H/\mathrm{d}t)\mathrm{d}t \Big/ \int_0^\infty (\mathrm{d}H/\mathrm{d}t)\mathrm{d}t \qquad (1)$$

taking $t=0$ at the moment of attainment of thermal equilibrium and $t=\infty$ at the end of crystallization[16]. Equating the integrals to areas, equation (1) can be shaped into:

$$x(t) = A_t/A_\infty \qquad (2)$$

A_t is the area under the d.s.c. curve from $t=0$ to $t=t$, and A_∞ is the total area under the crystallization curve. In a certain sense $x(t)$ is a reduced crystallinity because it relates an instant crystallinity to the total one which can be attained under the experimental conditions; therefore $x(t)$ changes from 0 to 1.

The plots of $x(t)$ vs. t, for each fraction and T_c are shown in *Figure 3*. The slopes of the curve at each point are a measure of the rate of crystallization. Beyond the induction period the rate of crystallization increases and then keeps constant for a certain time decreasing afterwards until zero value. We take V_c as the rate of crystallization, corresponding to the straight section of the curve[48]. This constancy is displayed over 50–60% of the conversion curve in all the experiments.

Table 1 shows the values of V_c corresponding to each T_c and molecular weight.

The activation energy associated to the overall process of crystallization has been evaluated from the rates of crystallization by using the equation:

$$V_c = A\exp(-\Delta E/RT) \qquad (3)$$

A being a constant and T the crystallization temperature T_c. The plot of ln V_c vs. T^{-1} allows the calculation of ΔE for each fraction from the slopes. The results are gathered in *Table 2*.

It can be observed that the lowest molecular weight fraction (*A*-4) has a large ΔE value compared with the highest molecular weight fraction (*A*-1), almost twice. The rest of the fractions have intermediate values.

In addition, taking the curves $x(t)$ vs. t, we have determined other parameters, such as $t_{0.5}$ and $t_{0.1}$, that is, the times when the reduced crystallinities get the values 0.5 and 0.1, respectively. The values obtained are given in *Table 1*, and their dependence on the molecular weight is shown in *Figure 4*.

The kinetic analysis of the isothermal crystallization was carried out on the basis of the Avrami equation[49]:

$$\theta(t) = 1 - x(t) = \exp(-Kt^n) \qquad (4)$$

Table 2 Activation energy values for the fractions

Fraction	$\bar{M}_n$	ΔE (kJ mol^{-1})
A – 1	11750	183.9
A – 2	8100	273.7
A – 3	7100	273.7
A – 4	5350	405.4
A – 0 (unfractionated)	6650	301.0

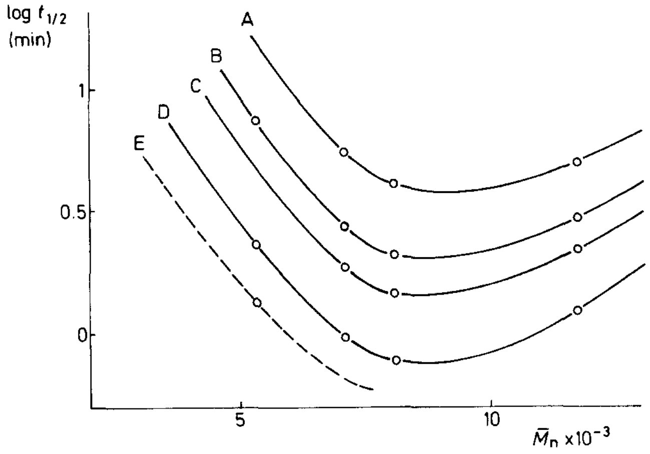

Figure 4 Plot of log $t_{0.5}$ vs. M_n for the various fractions, taking T_c as parameter. Curve A: T_c=508 K; curve B: T_c=505 K; curve C: T_c=503 K; curve D: T_c=500 K; curve E: T_c=498 K

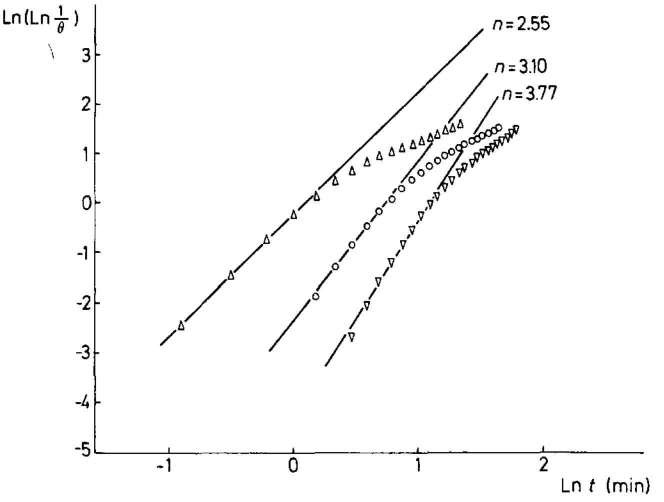

Figure 5 The Avrami equation for fraction *A*-3 (M_n=7100). Crystallization temperature as parameter: (△) 500 K, (○) 503 K, (▽) 505 K

$\theta(t) = 1 - x(t)$ being the weight fraction of uncrystallized material at time t, and K the rate constant. 'n' is a constant which depends both on the nucleation and growth of the polymer. The Avrami equation assumes that growth ceases at the onset of the impingement between growing bodies, 'n' was usually given integral values in order to permit theoretical interpretation. The Avrami equation can be rearranged into the known Göler–Sachs equations[50], at low degrees of conversion, which imply free growth.

Taking logarithms, equation (4) can be arranged in the following form:

$$\ln[-\ln\theta(t)] = \ln K + n \ln t \qquad (5)$$

Plotting the first term vs. $\ln t$, both K and n can be obtained, from the slope and intercept at $\ln t = 0$, respectively. Another way of obtaining the rate constant K is to use the half-life for crystallization $t_{0.5}$, by means of the equation:

$$K = \ln 2 / t^n_{0.5} \qquad (6)$$

Figure 5 shows a plot of equation (5) for a fraction crystallized at three different temperatures, and in *Table 1* the values of K and n are gathered for each fraction and T_c.

In order to establish a relationship between the various parameters and the undercooling ΔT, this has been evaluated by the equation:

$$\Delta T = T^\circ_m - T_c \qquad (7)$$

T°_m being the equilibrium melting temperature for each fraction, which has been determined by the relationship between the apparent melting temperature T_m and the crystallization temperature T_c. The plot of T_m vs. T_c gives straight lines whose crossing points with the line $T_m = T_c$ determine T°_m (*Figure 6*)[51].

The values of the overall crystallinity, x(%), obtained at the end of each crystallization kinetics are also given in *Table 1*. The range of x is between 45 and 75%, according to the fraction and crystallization conditions.

DISCUSSION

The induction time τ_i is clearly dependent on the crystallization temperature, for all the fractions studied, decreasing as the undercooling increases. This is a consequence of the smaller size for the critical nuclei required when the crystallization temperature is lower. With regard to the molecular weight, the strong dependence between τ_i and M_n when the undercooling is small and how this dependence becomes less pronounced at larger undercoolings can be observed in *Figure 2*. The τ_i values pass through a minimum at a molecular weight of about 9200. The observations can be explained by taking into account the effect of the viscosity and thermal agitation on the medium, both dependent as much as the molecular weight as the undercooling. At higher molecular weight the medium is more viscous, a condition which makes transport to the interface more difficult, thus increasing the induction time. For low molecular weights the viscosity is lower but thermal agitation opposes the formation of stable nuclei, which gives rise to higher induction times also. The molecular weight at which τ_i is a minimum shows the optimum conditions both in viscosity and thermal agitation and this implies formation of stable nuclei and easy transport to the interfaces. At lower crystallization temperatures and higher undercoolings, this effect will be less pronounced and the induction time becomes practically independent of the molecular weight.

The relationship between τ_i and ΔT can be represented by the equation:

$$\tau_i = \mathrm{const}(\Delta T)^{-n} \qquad (8)$$

and $\log \tau_i$ has been plotted vs. $\log \Delta T$. The average value of n for the fractions is 11.0 (*A*-*1* = 11.6; *A*-2 = 11.0 and *A*-*3* = 10.5). The observed linear dependence implies that there are no morphological changes during the crystallization as the undercooling varies[52].

As it was expected, the change of the reduced crystallinity $x(t)$ as a function of time is influenced by both the undercooling and the molecular weight (*Figure 3*). As the crystallization temperature rises the rate increases and overlapping of the curves cannot be obtained by a simple shift along the abscissae. This will cause larger apparent values of V_c and smaller ones for $t_{0.5}$ and $t_{0.1}$. In a similar

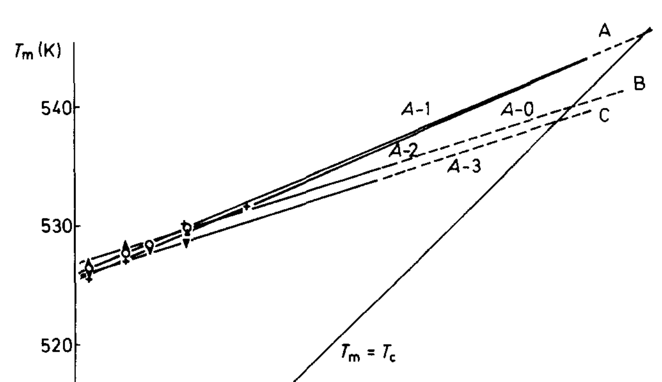

Figure 6 Determination of the equilibrium melting temperature T^0_m for several fractions. Curve A: 546 K; curve B: 539.8 K; curve C: 538.5 K

way, the molecular weight has an important influence, giving rise to variations in the rates and related parameters. In *Figure 4* the presence of either a maximum or a minimum, depending on the parameter, at a molecular weight of about 9200, as it happens with the induction time can be observed.

When the molecular weight increases, the rate of crystallization should decrease, as well as the density of the crystallized polymer and the final degree of crystallinity reached. The dependence of the velocity on the molecular weight is related both to the free energy of formation of the critical nucleus ΔF^* and to the free energy of transport at the interface liquid-crystal. ΔF^* is independent of molecular weight for large values[32,33], and the dominant term is the transport one, which is related to the viscosity of the melt. An increase of molecular weight causes an increase in the viscosity and this gives rise to constraints as far as the crystallization rate concerns. Nevertheless, for low molecular weight, ΔF^* will show a dependence on the molecular weight. As the crystallization temperature is getting lower the effect of the molecular weight will be less important because the size of the critical nucleus will be smaller and as a consequence the concentration of chain units required for nucleation will be lower.

In *Figure 4* it can be appreciated that each isotherm has a minimum for the half-life of crystallization in its relation to the molecular weight. This minimum shifts to lower values of molecular weight with decreasing crystallization temperatures. The initial lowering of $t_{0.5}$ with $\bar{M}_n$ is explained because of a decrease in the free energy required for the formation of a critical nucleus. The subsequent increase is due to the melt viscosity increase, which is related to the transport term (as ΔF^* does not depend on molecular weight).

The minimum is a result of both opposing tendencies as a function of molecular weight, one the decrease of ΔF^* and the other the increase of the transport term, related to the increase of viscosity. The shifting of $\bar{M}_n$ at the minimum, when the crystallization temperature lowers, is due to the smaller size of the critical nucleus required and therefore to the beginning of the independence of ΔF^* on the molecular weight. Also, as the T_c decreases, the viscosity increases and the transport term begins to be dominant at the lower molecular weight range. This effect has been observed in other polymers[27,53]. This minimum becomes more diffuse as the crystallization temperature decreases.

The activation energies, evaluated from the crystallization rates V_c and reported in *Table 2* for each fraction, are high. This is a consequence of the large cohesive energy density due to the rigidity of the chain and in the presence of polar groups. The values obtained are closely related to other data previously reported: Collier and Baer[54] give 267.5 kJ mol^{-1} (equal our fractions *A*-2 and *A*-3), Miller[41] and Mayhan[40] report 183.9 and 154.6 kJ mol^{-1}, respectively, for the higher molecular weights similar to that of our *A*-1 fraction.

The large difference between the activation energies of the smallest and largest molecular weight fractions, may be due to different crystallization mechanisms, similar to other polymers, such as poly-ε-caprolactone[55] and poly(ethylene oxide)[20]. The low molecular weight fractions (short chains) would assume a stretched conformation on crystallization (high activation energy) while the high molecular weight fractions would crystallize with a folded chain conformation, which is more favourable from a kinetic point of view (low activation energy). As a consequence, the low molecular weight fractions would crystallize with low rates. The higher the molecular weight of the fraction the longer the chain, making chain folding easier, the activation energy will decrease and therefore the crystallization rate will be higher (fractions *A*-3 and *A*-2). Nevertheless, the chains do not have enough flexibility for a rapid crystallization even when there was an increase in the rate. At higher molecular weights the long chain lengths offer more favourable conditions for folding, the rate of crystallization ought to be better and the corresponding activation energies would be low. But the ease of folding is limited by the viscosity of the medium, which increases with the molecular weight. This opposes the higher crystallization rates and the final crystallization rate would be less than expected due to the low activation energies. This would explain the maximum found when plotting the crystallization rate vs. molecular weight.

Values of the exponent n in the Avrami equation range from 2–4, for every fraction studied, and decrease, as expected, with increasing undercoolings. In nearly all of the experiments the n values obtained are non-integer. This happens with other polymers, e.g. polyethylene[8,56], poly(ethylene oxide)[20,57], poly(decamethylene terephthalate)[30], etc., and can be ascribed to heterogeneous nucleation.

The rate constant K rises with increasing undercoolings, as expected. With regard to the molecular weight, the data show the presence of a maximum when plotting ln K vs. $\bar{M}_n$. This same effect has been reported by Magill with other polymers[53]. The $\bar{M}_n$ corresponding to the maximum is the same as that found in the crystallization rate analysis and corresponds to the minimum in the study of the half-lives of crystallization. However, the molecular weight corresponding to the maximum on the K plot, for a given T_c, shifts to higher values as T_c increases, e.g. for a $T_c = 500$ K the molecular weight is 8750, and when $T_c = 508$ K it is 9750.

As the growth of the crystalline entities takes place by a process of secondary nucleation on the faces of initially formed nuclei, the dependence of K with the molecular weight must be related to both the free energy of nuclei formation and the transport energy on the liquid-crystal interface. The molecular weight will affect all these quantities, as will the crystallization temperature. This explains the presence of the maximum and its shifting along the molecular weight axis.

The relationship between K and the undercooling may be explained if the secondary crystallization associated with the growth of the crystal is either bidimensional or tri-dimensional. In this case, a linear relationship between either log K and $(\Delta T)^{-1}$ or log K and $T_m/T(\Delta T)$ points to growth from secondary bidimensional nuclei, while a linear relationship between log K and $(\Delta T)^{-2}$ or between log K and $T_m/T(\Delta T)^2$ is a clear indication of tridimensional secondary nuclei responsible for growth.

It can be seen that a linear relationship exists in every case and so it is impossible to distinguish between both types of secondary nucleation. These difficulties have been dealt with previously by other authors[1,2]. But the problem can be solved by analysing the temperature coefficient, as will be shown later.

ACKNOWLEDGEMENT

One of the authors (P.C.V.) wishes to express his thanks to the Ministerio de Educación y Ciencia for a Beca de Formación de Personal Investigador during the course of the present study.

REFERENCES

1 Mandelkern, L. in 'Crystallization of Polymers', McGraw-Hill, New York, 1964
2 Sharples, A. in 'Introduction to Polymer Crystallization', Edward Arnold Ltd, London, 1966
3 Bekkedahl, N. *J. Res. Natl. Stand.* 1949, **42**, 145
4 Mandelkern, L. and Flory, P. J. *J. Am. Chem. Soc.* 1951, **73**, 3206
5 Flory, P. J., Mandelkern, L. and Hall, H. K. *J. Am. Chem. Soc.* 1951, **73**, 2532
6 Mandelkern, L., Quinn, F. A. and Flory, P. J. *J. Appl. Phys.* 1954, **25**, 830
7 Baker, C. H. and Mandelkern, L. *Polymer* 1966, **7**, 7
8 Banks, W., Gordon, M., Roe, R. J. and Sharples, A. *Polymer* 1963, **4**, 61
9 Banks, W., Hay, J. N., Sharples, A. and Thomson, G. *Polymer* 1964, **5**, 163
10 Booth, A. and Hay, J. N. *Polymer* 1971, **12**, 365
11 Pella, E. and Ne buloni, M. *J. Therm. Analy.* 1971, **3**, 229
12 Gopalan, M. and Mandelkern, L. *J. Phys. Chem.* 1967, **12**, 3823
13 Inoue, M. *J. Polym. Sci. A-1* 1963, **1**, 2697
14 Fatou, J. M. G. and Barrales-Rienda, J. M. *J. Polym. Sci. A-2* 1969, **7**, 1755
15 Barrales-Rienda, J. M. and Fatou, J. M. G. *Polymer* 1972, **13**, 407
16 Mancarella, C. and Martucelli, E. *Polymer* 1977, **18**, 1240
17 Hay, J. N. and Mills, P. J. *Polymer* 1982, **23**, 1380
18 Hay, J. N. *J. Polym. Sci. A-3* 1965, **4**, 433
19 Beech, D. R., Booth, C., Hillier, I. H. and Picles, C. J. *Europ. Polym. J.* 1972, **8**, 799
20 Godovsky, Yu., Slonimsky, G. L. and Garbar, N. M. *J. Polym. Sci. Polym. Symp.* 1972, **37**, 1
21 Magill, J. H. *Polymer* 1961, **3**, 221; *Nature* 1961, **191**, 1092
22 Kolb, H. J. and Izard, E. F. *J. Appl. Phys.* 1949, **20**, 571
23 Booth, A. and Hay, J. N. *Polymer* 1969, **10**, 95
24 Hay, J. N., Wiles, M. and Fitzgerald, P. A. *Polymer* 1976, **17**, 1015
25 Mandelkern, L., Fatou, J. M. G. and Ohno, K. *J. Polym. Sci. B* 1968, **6**, 615
26 Ueberreiter, K., Kanig, G. and Brenner, A. S. *J. Polym. Sci.* 1959, **16**, 53
27 Ergoz, E., Fatou, J. M. G. and Mandelkern, L. *Macromolecules* 1972, **5**, 147
28 Turska, E. and Gogolewski, S. *J. Appl. Polym. Sci.* 1975, **19**, 637
29 Parrini, P. and Corrieri, G. *Makromol. Chem.* 1963, **62**, 83
30 Sharples, A. and Swinton, E. L. *Polymer* 1963 **4**, 119
31 Fatou, J. M. G. and Mandelkern, L. *J. Phys. Chem.* 1965, **64**, 417
32 Mandelkern, L., Fatou, J. M. G. and Howard, C. *J. Phys. Chem.* 1964, **68**, 3386
33 Mandelkern, L., Fatou, J. M. G. and Howard, C. *J. Phys. Chem.* 1965, **69**, 956
34 Marco, C., Fatou, J. M. G., Bello, A. and Blanco, A. *Polymer* 1979, **20**, 1250
35 Tinas, J. and Fatou, J. M. G. *An. Quim* 1980, **76**, 3
36 Cobbs, W. H. and Burton, R. L. *J. Polym. Sci.* 1953, **10**, 275
37 Zachmann, H. G. and Stuart, H. A. *Makromol. Chem.* 1960, **41**, 131
38 Turska, E. and Przygochi, W. *J. Polym. Sci. C* 1968, **16**, 3373
39 Keller, A., Lester, G. R. and Morgan, L. B. *Phil. Trans. Roy. Soc. London* 1954, **A-247**, 1, 23
40 Mayhan, K. G., James, W. J. and Bosch, W. *J. Appl. Polym. Sci.* 1965, **9**, 3605
41 Miller, B. *J. Appl. Polym. Sci.* 1967, **11**, 2343
42 Mitsuishi, Y., Ikeda, M. *J. Polym. Sci. A-2* 1966, **4**, 283
43 Gilbert, M. and Hybart, F. J. *Polymer* 1972, **13**, 327
44 Van Antwerpen, F. 'Kinetics of Crystallization Phenomena of Spherulites in PET', Tesis Doctoral, Nijmegen, 1971
45 Baranov, V. G., Keranov, A. V. and Volkov, T. I. *J. Polym. Sci. C* 1970, **30**, 271
46 Colomer, P., Montserrat, S. and Guzman, G. M. *An. Quím.* 1983, **79**, 320
47 Roberts, R. C. *Polymer* 1969, **10**, 113
48 Knox, J. R. 'Analytical Calorimetry' (Eds. R. S. Porter and J. F. Johnson), Plenum Press, New York, 1968, Vol. 1, p. 45
49 Avrami, M. *J. Chem. Phys.* 1939, **7**, 1103; 1941, **9**, 177
50 Göler, V., Sachs, F. and Sachs, G. *Z. Phys.* 1932, **77**, 286
51 Hoffman, J. D. and Weecks, J. *J. Res. Natl. Bur. Stand.* 1962, **66A**, 13
52 Kantrovitz, A. *J. Chem. Phys.* 1951, **19**, 1097
53 Magill, J. H. *J. Polym. Sci. B* 1968, **6**, 853
54 Baer, I., Collier, J. R. and Carter, D. R. *SPE Trans.* 1965, **5**, 22
55 Perret, R. and Skoulios, A. *Makromol. Chem.* 1972, **156**, 157
56 Banks, W. and Sharples, A. *Makromol. Chem.* 1963, **59**, 233
57 Hillier, I. H. *J. Polym. Sci. A-2* 1965, **3**, 3067; 1966, **4**, 1